https://doi.org/10.5194/egusphere-2022-31
Preprint. Discussion started: 10 March 2022

Upper Ocean Response on the Passage of Tropical Cyclones in the Azores Region

Miguel M. Lima[1] (malima@fc.ul.pt), Célia M. Gouveia[1,2] (cmgouveia@fc.ul.pt), Ricardo M. Trigo[1,3] (rmtrigo@fc.ul.pt)

Correspondence to: Miguel M. Lima (malima@fc.ul.pt)

[1]Instituto Dom Luiz (IDL), Faculdade de Ciências, Universidade de Lisboa, 1749-016, Lisboa, Portugal
[2]Instituto Português do Mar e da Atmosfera (IPMA), I.P., 1749-077, Rua C do Aeroporto, Lisboa, Portugal
[3]Departamento de Meteorologia, Universidade Federal do Rio de Janeiro, Rio de Janeiro 21941-919, Brasil

Abstract. Tropical Cyclones (TCs) are extreme climate events that are known to strongly interact with the ocean through two mechanisms: dynamically through the associated intense wind stress, and thermodynamically through moist enthalpy exchanges at the ocean surface. These interactions contribute to relevant oceanic responses after the passage of a TC, namely the induction of a cold wake and the production of chlorophyll (chl-a) blooms. This study aimed to understand these interactions in the Azores region, an area with relatively low cyclonic activity for the North Atlantic basin, since the area experiences much less intense events than the rest of the basin. Results for the 1998-2020 period showed that the averaged induced anomalies were on the order of +0.026 mg/m^3 for the chl-a and -1.554 K for SST. Furthermore, looking at the role played by several TCs characteristics we found that the intensity of the TCs was the most important condition for the development of upper ocean responses. Two other analysed conditions were the TC's translation speeds and the impacted areas, which also showed to be positively affecting the registered induced anomalies. Two case studies (Ophelia, in 2017, and Nadine, in 2012) were conducted to better understand each upper ocean response. Ophelia showed to affect the SST at an earlier stage while the biggest chl-a induced anomalies were registered at a later stage, allowing the conclusion that thermodynamic exchanges conditioned the SST more while dynamical mixing played a more important role in the later stage. Nadine showed the importance of the TC track geometry, revealing that the TC track observed in each event can impact a specific region for longer, and therefore induce greater anomalies.

Introduction

Tropical Cyclones (TCs) are potentially intense atmospheric disturbances which are characterised by a low-pressure centre (eye) where strong winds curl around. Among other important properties, TCs are thermodynamic dependent phenomena, meaning that intense temperature gradients need to occur in the lower atmosphere to maintain and intensify the storm. Thus, TCs are fed from warm sea water which provide a strong moist enthalpy flux from the oceanic surface to maintain a steep temperature gradient within the lower and middle troposphere and produce massive water vapour convection (Emanuel, 2003; Holton & Hakim, 2012; Pearce, 1987).

https://doi.org/10.5194/egusphere-2022-31
Preprint. Discussion started: 10 March 2022

The strong wind stress present near the surface and the associated intense curl are also shown to induce vertical mixing and Ekman upwelling in the upper layer of the ocean. In the seminal study by Price (1981) it is shown, through both observed and numerical modelling data, the evolution of sea surface temperature (SST) on the passage of a hurricane, with the emergence of a cold wake of SST after a TC due to entrainment of water from shallow layers. This effect has since been well studied and documented with many case studies observed, for example, the case of Hurricane Felix, in the vicinity of Bermuda in 1995, that showed decreases in the order of 3.5-4 ºC (Dickey *et al.*, 1998), or the cases of cyclones Nargis (2008) and Laila (2010), in the Bay of Bengal, that caused SSTs to drop by around 1.76 ºC (Maneesha *et al.*, 2012). Additionally, several model-based works have been done either according to the effect caused by the TCs, as well as the interaction of the TC with its own cold wake (e.g., Chen *et al.*, 2017; Zhang *et al.*, 2019).

There are also biological responses to the passage of a TC. Due to the upwelling of colder water, there may also occur the transport of nutrient-rich water from the sub-superficial layer (Kawai & Wada, 2011). In this case, phytoplankton can quickly increase in the surface layer following the rise in nutrients. This increase can be remotely sensed through satellite observations that capture the chlorophyll-a concentration (Chl-a) increasing after the passage of a TC, since chl-a is generally accepted as a proxy for biological activity (Kawai & Wada, 2011; Liu *et al.*, 2009; Subrahmanyam *et al.*, 2002; Walker *et al*., 2005).

The oceanic response, either physical or biological, to the passage of a TC depends on various aspects, most remarkably the TC's intensity and its translation speed but also the oceanic subsurface conditions (Zheng et al., 2008). The magnitude and significance of these aspects on the modulation of the oceanic response varies regionally, although it is generally regarded that the most impactful phenomena to be those of an intense and slow TC (Chacko, 2019; Price, 1981; Price et al., 1994). Recent studies (e.g., Chacko, 2019; Pan et al., 2018; Shropshire et al., 2016) have shown that regional differences do matter when studying the biological response. In the case of the Bay of Bengal, it was shown that the intensity of a TC is less important, and the most meaningful aspects are the TC's translation speed and, to a lesser degree, a pre-existing shallow mixed layer (Chacko 2019). The results from this study are important to stress that relatively weaker TCs can also induce a strong biological response after their passage.

Until now, the Azores region has not been studied regarding its thermodynamic and biological impacts. This section of the North Atlantic basin presents much fewer and weaker cyclones than the tropical band of the basin, with this region being mainly a zone where TCs undergo either cyclosis or post-tropical transition into extra-tropical cyclones or mid-latitude storms (Baatsen et al., 2015; Haarsma et al., 2013). The north-eastern Atlantic (NEA) basin, where the Azores archipelago is located, presents significantly less TCs than the western counterpart, closer to the USA coast (Baatsen et al., 2015; Lima et al., 2021; Haarsma et al., 2013). However, there is growing evidence of a significant increase in the frequency of strong TCs in both western (Kossin et al., 2020) and eastern (Lima et al., 2021) halves of the north Atlantic Ocean. The climatology of the area points to a south-north gradient in both SST and chl-a, with a decrease in the former and an increase in the latter (Amorim et al., 2017). In general, the southern part of the Azores region offers SSTs high enough to maintain TCs, although the necessary atmospheric conditions (e.g., high lapse rates and low wind shear) need to occur for their passage northeast through the Azores (Lima et al., 2021). However, this area is undergoing a transition due to anthropogenic climate change and an increase both in number and intensity of TCs is expected (Baatsen et al., 2015; Haarsma et al., 2013). Therefore, the NEA basin is a challenging study region to assess the impact that lower intensity TCs have on the oceanic surface.

The main aim of this study is to analyse in detail the upper ocean response observed after the passage of a TC in the Azores region, which is characterised by its lower-than-normal cyclonic activity in relation to the rest of the north Atlantic basin. In particular, we aim to evaluate the impacts on sea surface temperature (SST) and chlorophyll-a concentration (Chl-a) produced by three important TC characteristics (averaged maximum wind speed, cumulative impacted area, and average translation speed). Two practical case studies, relative to Nadine (2012) and Ophelia (2017) are then thoroughly analysed to reflect the drawn conclusions for this area.

Data

Data used to evaluate the oceanic response in this study is divided into three main parts: Remotely sensed data used to characterise the chl-a and SST, respectively, and TC track data, which provides the necessary additional information on the location and dynamic variables of each TC, that allow to explore the oceanic response in the aforementioned data.

Biological oceanic response was evaluated using a multi-sensor daily chl-a product available through the Copernicus Marine Environment Monitoring Service (CMEMS) in a 4 km x 4 km resolution from the end of 1997 to the present (CMEMS, 2021b). This product, delivered by the ACRI-ST company, is based on the Copernicus-GlobColour project and obtained by merging different sensors: SeaWiFS, MODIS, MERIS, VIIRS-SNPP&JPSS1, OLCI-S3A&S3B. The final chl-a product is a mix of several algorithms that consider different water conditions, such as oligotrophic, mesotrophic, coastal, clear, and complex waters (Garnesson et al., 2019). To produce a "cloud free" product, the resulting data was subjected to daily interpolation to fill any gaps (Krasnopolsky et al., 2016; Saulquin et al., 2019). The lack of gaps in this dataset is particularly relevant in the context of this study since the areas analysed will be concentrated around the TCs; it is then expected that large amounts of the analysed areas would be under cloud coverage and, therefore, some of the analysed data is not real but interpolated values.

To evaluate the physical oceanic response and to relate this to the biological one, a daily SST dataset from the CMEMS was used, with a 0.05º resolution. This data is available from 1981 up to the near present (CMEMS, 2021a). Similarly, to the previous chl-a product the SST field is also a blended gap-free analysis product, with the present one resulting from re-processed (A)ATSR, SLSTR and AVHRR sensor data being applied to the Operational SST and Sea Ice Analysis (OSTIA) system (Donlon et al., 2012). This reprocessed analysis product provides an estimate of the SST at 20 cm depth. The inputs to the system are SSTs at 10:30 am and 10.30 pm local time which means that the analyses roughly correspond to the daily average SST (Good et al., 2020; Lavergne et al., 2019; Merchant et al., 2013).

The TC track data is made available by the *International Best Track Archive for Climate Stewardship Project* version 4 (IBTrACS v4) free access dataset (Knapp *et al.*, 2009). This dataset contains global information regarding TC

https://doi.org/10.5194/egusphere-2022-31
Preprint. Discussion started: 10 March 2022

activity since the 1851 hurricane season up to the most recent full hurricane season, 2020. It aggregates variables such as TC geographical location, maximum wind speed, minimum sea level pressure, and storm radius estimation based on wind intensity, measured at 6-hour intervals (original dataset interpolates for increased resolution, at 3-hour rates, however this interpolation only includes the geographical location). For the 1998-2020 period, the Azores region experienced the passage of 62 individual TCs accounting to 642 6-hour observations that are categorised in the following intensities according to the Saffir-Simpson hurricane wind scale (Taylor *et al.*, 2010):

- 148 tropical depression observations.
- 389 tropical storm observations.
- 85 category 1 hurricane observations.
- 18 category 2 hurricane observations.
- 2 category 3 hurricane observations.

The TC tracks can be better visualised in Fig. 1, with the left panel showing the full track for all these 62 TCs' observed in the NA basin for the 1998-2020 period and the right panel shows a zoomed view relative to the considered Azores region. Tropical depression observations (dark blue in Fig. 1, right panel) account for 23 % of the total observations and will not be considered in this study, as they present the lower branch of intensities with winds below the 34-kt (18 m/s) threshold. Therefore, a total of 494 TC 6-hour observations were considered for this study.

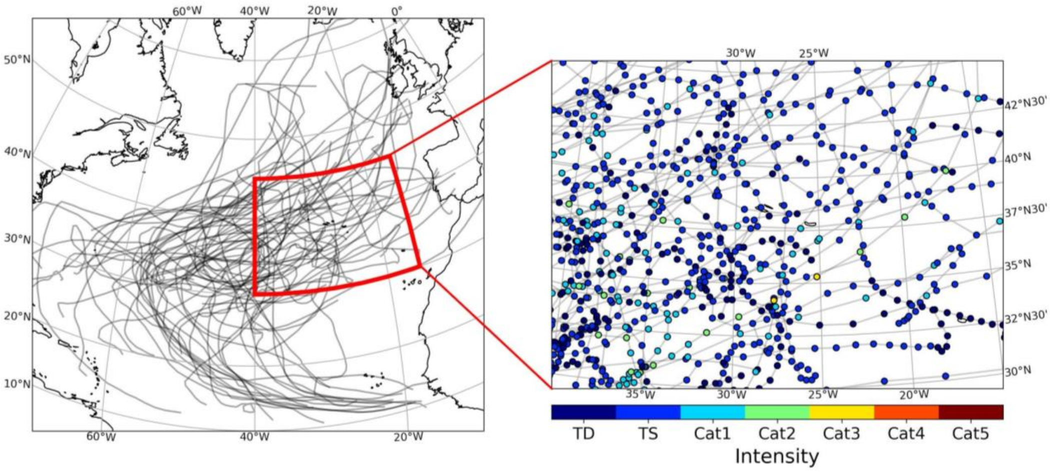

Figure 1 - Left panel: North Atlantic basin and the tracks for all TCs that went through or occurred inside the study region (shown by the red outline). Right panel: Zoom of the previous red outline, with each TC observation marked in different colours for intensity (TD: Tropical Depression; TS: Tropical Storm; Cat1 - Cat5: Hurricane category according to the hurricane Saffir-Simpson wind scale).

Since the datasets do not share the same time frame and to better encapsulate full years of data, the timeframe of the present study will be from January 1st of 1998 to December 31st of 2020. Moreover, while we have extracted all the

https://doi.org/10.5194/egusphere-2022-31
Preprint. Discussion started: 10 March 2022

data described above covering the entire North Atlantic basin, we will focus on the area around the Azores archipelago, delimited by the 15ºW and 40ºW meridians and between the 30ºN and the 45º parallels.

Methodology

The area of focus on this study is centred in the Azores archipelago in the North Atlantic basin, pictured in Fig. 1. The area is longitudinally delimited by the 15ºW and 40ºW meridians and latitudinally between the 30ºN and the 45º parallels. This region was chosen due to its nature regarding TCs, since it is an area with less quantity and intensity of tropical storms (Hart & Evans, 2001; Lima et al., 2021; Ramsay, 2017). Generally, tropical cyclosis and post-tropical transition occurs here (Baatsen et al., 2015; Haarsma et al., 2013). Because of these aspects, it corresponds to a much less studied area and is a good region to characterise oceanic bio-physical effects after the passage of (generally) weaker TCs at higher-than-tropical latitudes, and to compare the obtained results with previous literature.

To cope with large amounts of data, the bio-physical response was evaluated within a small area around individual locations obtained for each TCs' best-track location. For this, we used the approximated quadrant radius given by the IBTrACS v4 dataset. This dataset provides different types of radii depending on the considered isotach, for this study we used the 34-kt isotach as it corresponds to the lower-bound for the Tropical Storm status according to the Saffir-Simpson hurricane wind scale (Taylor et al., 2010). Since the considered area of analysis would be above the 34-kt isotach, any tropical depression observation was not considered (exact partition of intensities is given at the beginning of the *Results* section). To correct some missing radii values in the middle of TC tracks, a simple linear regression was applied. An example of this methodology can be observed in Figs. 6a and 7a, for hurricanes Ophelia (2017) and Nadine (2012), respectively. From inside this area of analysis, we may retrieve the chl-a concentration and SST at their respective resolution, as well as study their anomalies and post-storm responses. The analysis inside the considered area is made recurring to histograms, in which each pixel inside the 34-kt isotach contributes to that TC's observation histogram.

To analyse the TCs' impact on their passage, a different approach was taken than the typical anomaly analysis since the effects caused by a TC may not be visible in simple anomalies computed against climatology. Some authors suggest that an appropriate time window to analyse the maximum bio-physical oceanic response would be approximately circa 10 days after the passage of a TC (Kawai & Wada, 2011). To assess the best temporal window for our region, we analysed the daily anomalies registered between 30-days before and 30-days after the passage of a TC. Afterwards, we chose two time windows to reflect different situations (Fig. 2): (a) An average, before the storm, situation, which is required to assess the oceanic conditions before the TC occurred in the area (i.e., average of red circles in Fig. 2, resulting in yellow circle); (b) And secondly, a time-window after the TC passed over the area, impinging the most significant response (Green circles, Fig. 2). Based on these definitions the induced anomaly can be calculated (blue circles, Fig. 2) by subtracting each daily value of (b) from the average situation before the storm described in (a). In the end, this leaves us with a large pool of observed daily induced anomalies to study, from which we may study the responses according to different TC intensities, translation speeds, or affected area.

https://doi.org/10.5194/egusphere-2022-31
Preprint. Discussion started: 10 March 2022

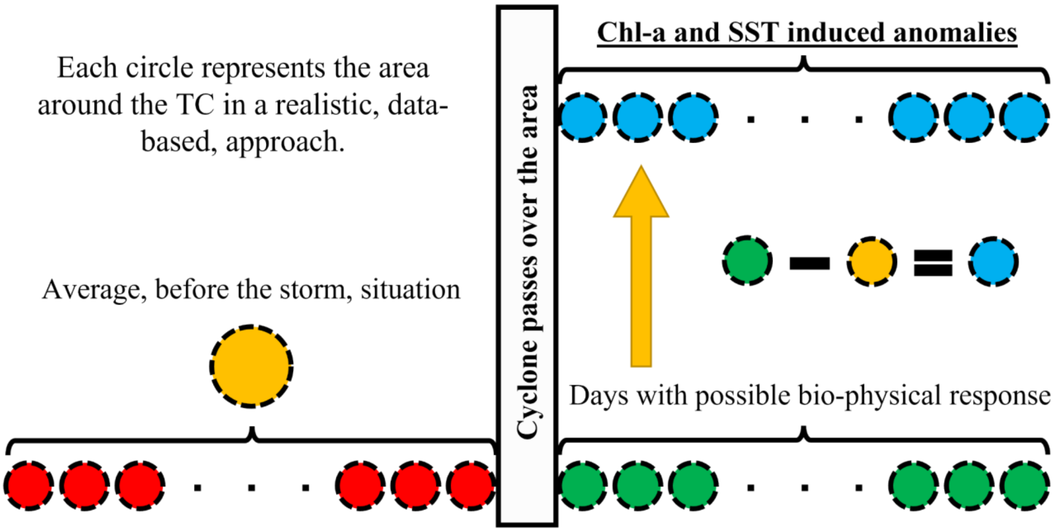

Figure 2 - Resumed schematic of the applied methodology in each TC observation. Do note that the circles are a mere representation of each affected area. The colour coding follows: Red – Individual daily observations before the TC; Green – Individual daily observation after the TC passes over the region; Yellow - Averaged values before the TC; Blue – Individual daily induced anomalies. A more detailed description of the methodology is presented in the text.

To address the possibility that some pixels are overlaid on top of each other, which would contaminate the analysis, as observed in the case of the slow erratic Hurricane Nadine (track seen in Fig. 7a), we did not take into consideration the days in which the TC is over the aforementioned overlaid region. Therefore, the days considered are those after the cyclone completely travelled over these areas.

To identify the appropriate time periods in this analysis we used a linear kernel change point detection algorithm that detects changes in the mean of any given signal (Celisse et al., 2018; Truong et al., 2020). Figure 3 shows the daily distribution of the Chl-a (Fig. 3a) and SST (Fig. 3b) anomalies 30 days before and after the TC passed over a given area. Using the change point detection algorithm, we identified 2 main periods associated with this passage: i) 7 to 16 days before the TC, representing an average condition prior to the arrival of the TC; ii) from 1 to 10 days after the period where it is clearly visible the effects on the oceanic variables. It is important to note that more periods were identified in between and after those presented due to the sensitivity of the algorithm but were not considered in the analysis for being too small or not showing relevance in our study (e.g.: from -17 to -30 days, or -4 to +1 days). The main 2 identified periods coincided in both cases (Figs. 3a and 3b), while those extra periods varied both in number and location.

https://doi.org/10.5194/egusphere-2022-31
Preprint. Discussion started: 10 March 2022

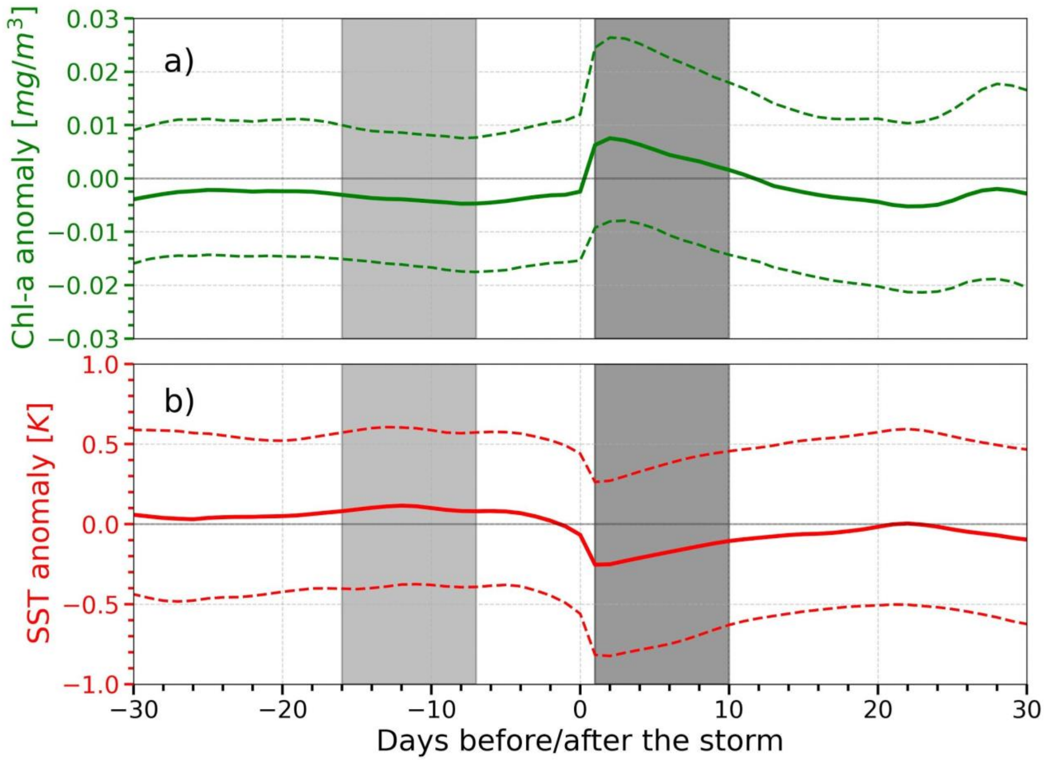

Figure 3 - Average daily a) chl-a (green solid line) and b) SST (red solid line) anomalies registered in a month period before/after each TC observation. Dotted lines show the first and third quartiles of each day. Shaded light grey area represents the period (-16 to -7 days) considered for the computation of the average before the storm situation and the darker grey represents the time period (+1 to +10 days) used to compute the induced anomalies.

Results and Discussion

Applying the mentioned methodology leaves us with a large pool of induced anomalies, from which we can now evaluate the distribution of anomalies for both the chl-a and SST as shown in Figs. 4a and 4b in the form of histograms of induced chl-a and SST anomalies, respectively. Both variables suffered a large impact after the passage of TCs, with the chl-a presenting a mean response of positive 0.026 mg/m^3 and the SST showing a mean response of negative 1.554 K. Figs. 4c-f show the corresponding distributions as a function of the cyclone's intensities (Figs. 4c and 4d) and translation speeds (Figs. 4e and 4f). To make these distinctions, we chose only the high values (either regarding intensity or translation speed) to be those above the third quartile and the lower values to be those below the second quartile.

https://doi.org/10.5194/egusphere-2022-31
Preprint. Discussion started: 10 March 2022

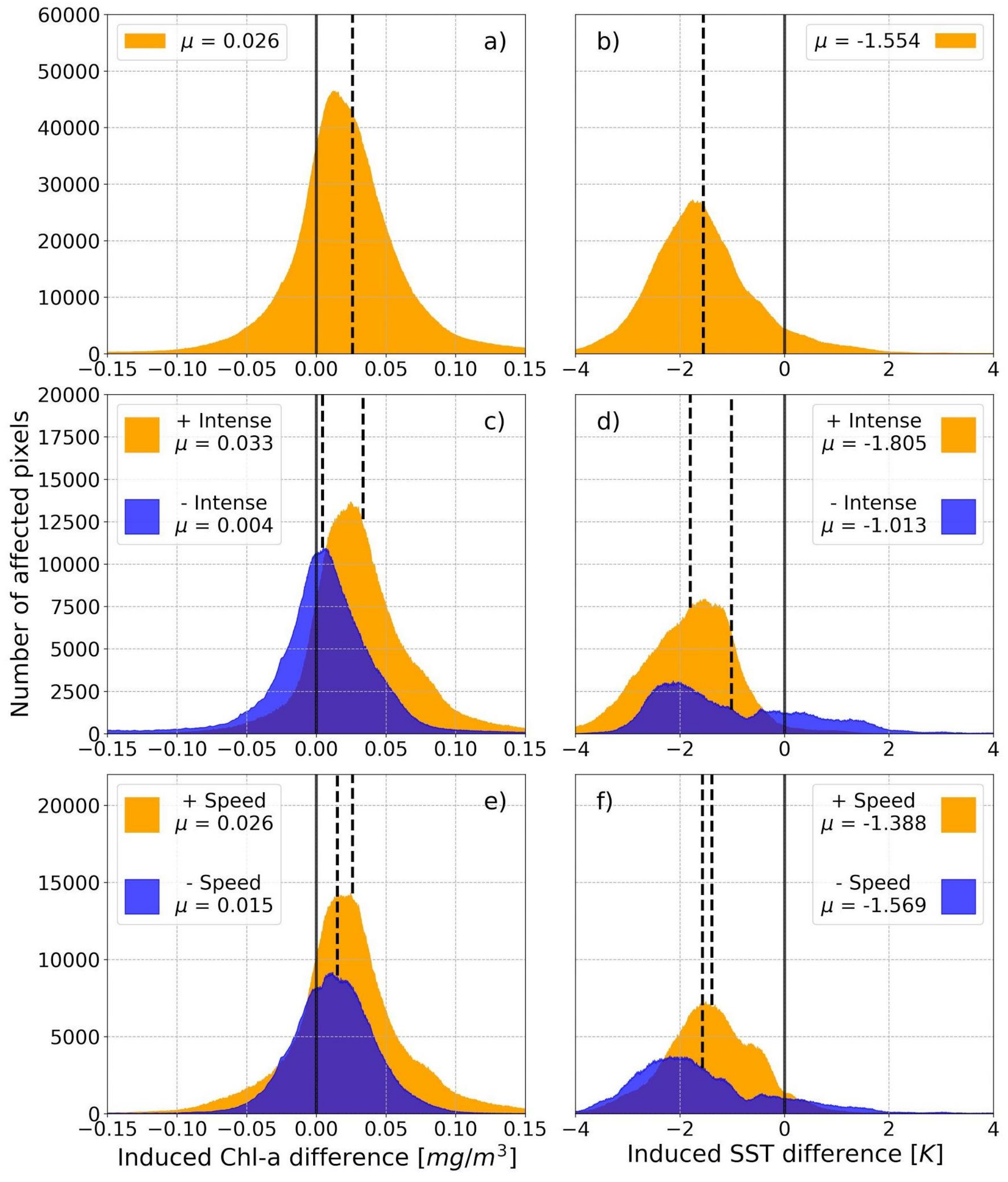

Figure 4 - Histograms for the: a) Total chl-a and b) SST induced anomalies; c) Chl-a and d) SST induced anomalies after weaker (blue) and powerful TCs (orange); e) Chl-a and f) SST induced anomalies after slow TCs (blue) and fast TCs (orange). Each subplot histogram presents the respective population mean value (μ) in a dashed black line, and the zero value on a grey line.

https://doi.org/10.5194/egusphere-2022-31
Preprint. Discussion started: 10 March 2022

Firstly, regarding intensity (Figs. 4c and 4d), we have the induced response of the most powerful intensities in orange and the weaker ones in blue. Regarding the impact as a function of intensity it is possible to observe that more powerful TCs tend to induce a stronger biological response than weaker ones, which have a mean response much closer to zero. It is also important to note that the more powerful TCs have a response that is much more skewed towards extreme positive values of chl-a. Fig. 4d, shows a much larger impact regarding different intensities in SST, in which even weaker TCs show a substantial mean response of -1.013 K and nearly all the analysed pixels showing negative induced anomalies. Important to note the nearly bimodal nature of this distribution, which can be attributed to both the earlier phase of TCs (more energy being drawn from the ocean) resulting in more negative SST values, and the less negative corresponding to the latter part of TCs since baroclinic instabilities are more prevalent than the action of moist enthalpy flux from the ocean at this phase (Baatsen et al., 2015; Emanuel, 2003). Powerful TCs induced a more varied distribution of anomalies, with a mean response of -1.805 K. Do note that these different distributions do not represent the same geographical areas, since they are analysing different observations associated with the location of each TC as it moves along its storm-track.

Regarding the different translation speeds, Fig. 4e shows that, for biological responses, this categorization is not as important since they present similar mean responses, close to the general one seen in Fig. 4a, with faster TCs showing a slightly larger mean value. On the other hand, the SST response (Fig. 4f) seems to be impacted by the TC's translation speed, with slower TCs having a stronger impact than faster ones. Even though the mean response values do not differ as much as the ones in Fig. 4d, these distributions show relatively greater deviations. Additionally, even if faster TCs do not affect the SST response as much as slower ones, the mean value is still close to what is seen in the general case in Fig. 4b, and most of the impact is towards negative SSTs.

To quantify these relations, Fig. 5 shows the storm-averaged induced anomalies compared to the averaged maximum wind, cumulative impacted area, and average translation speed. The linear regression is also shown for each of the comparisons, with all results significant at the 95 % statistical level except for those in the last column (regression line dashed). According to these plots, only the translation speed (Figs. 5c and 5f) did not show a significant relation with the chl-a and SST induced anomalies, at the 95 % statistical confidence level. Regarding the mean wind (Figs. 5a and 5d), and therefore the TC's average intensity within the Azores region, the linear regression showed significantly high values, upwards of 0.5. In the case of chl-a, like observed in Fig. 4, the relation is positive while with SST this relation is negative. The cumulative area (Figs. 5b and 5e) also presents a significant relation, although less intense than that observed with the mean winds. However, it should be noted that this variable is somewhat connected with the mean winds, since more intense cyclones tend to be larger than less powerful ones, but also with the storm phase, since storms nearing their post-tropical transition tend to grow larger (Knaff et al., 2014). It is then relatively straightforward that, in the Azores region, the variable that better relates the bio-physical oceanic response to the passage of a TC is its intensity (Figs. 4 and 5), and to a lesser degree its translation speed (Fig. 4).

https://doi.org/10.5194/egusphere-2022-31
Preprint. Discussion started: 10 March 2022

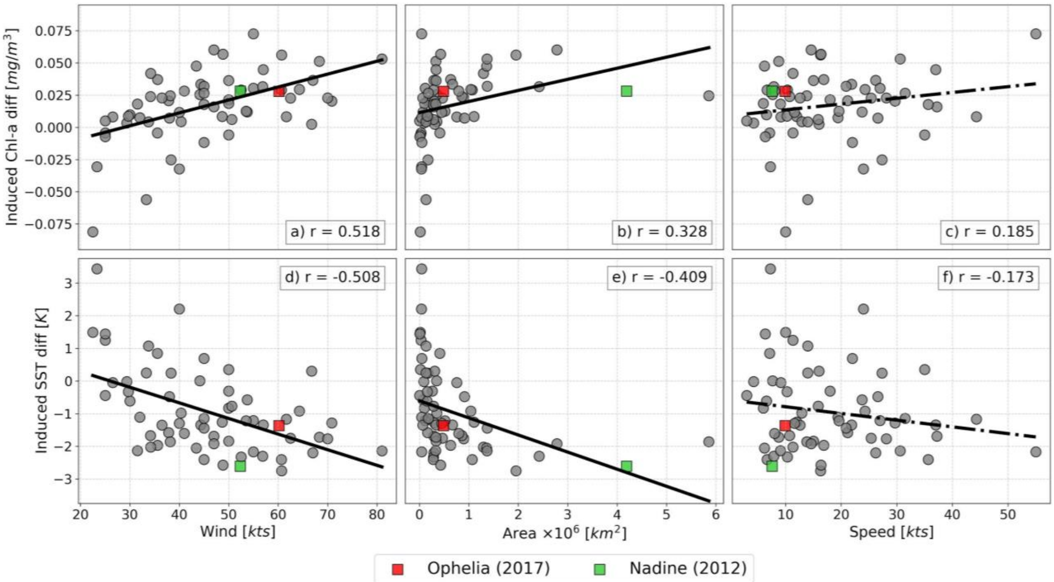

Figure 5 - Linear regression of chl-a (top panel) and SST (bottom panel) induced anomalies for each TC, respectively, when compared with: average winds in knots (left column); cumulative impacted area in km^2 (middle column); and average TC translation speed in knots (right column). In each plot the Pearson R is presented, and the regression's significance is marked by the type of line used in the regression, with a dashed line representing non-significant at a 95 % confidence level.

Still in Fig. 5, two case studies are marked: Hurricane Ophelia in 2017 (red square) and Hurricane Nadine in 2012 (green square). These case studies were chosen based on the presented characteristics, coupled with the amount of sampling within the region. Hurricane Ophelia (2017) was chosen due to its large intensity in the region (Red square in Fig. 5), reaching a category 3 intensity in the Saffir-Simpson hurricane wind scale, something abnormal for the region (Lima *et al.*, 2021). The complete TC track can be seen in Fig. 6a inset. Besides the large intensity, Ophelia's genesis took place inside our sector which enabled us to study different phases of the storm and its impacts on the ocean surface in the region. Even though hurricane Ophelia was so intense, this storm impacted a very small area (Figs. 5b and 5e) particularly when compared with the other case study, Hurricane Nadine (2012). Hurricane Nadine (Fig. 7a) was chosen due to its large sampling, relatively high intensity (maximum category 1) and massive impact area (second largest in this study). The large, impacted area was amplified by the geometry of the storm's track (i.e., many overlaid observations). Only the final stage of Hurricane Nadine was caught within the study region, producing an ideal case study to analyse the impact of a less intense storm that heavily impacted a particular region due to its geometry.

https://doi.org/10.5194/egusphere-2022-31
Preprint. Discussion started: 10 March 2022

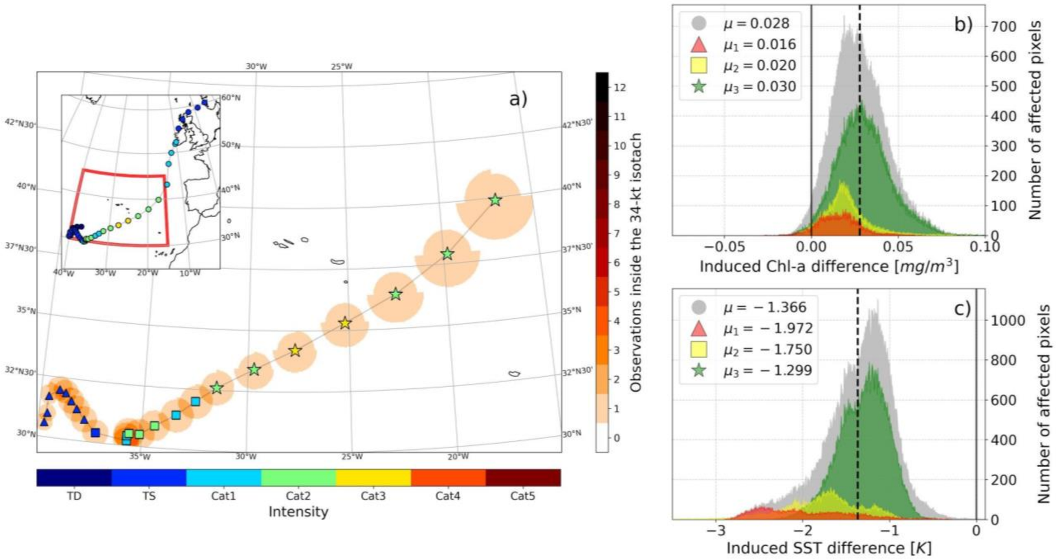

Figure 6 - Case study for Hurricane Ophelia, in 2017, with its track on the left panel (intensity colour scheme as in Fig. 2), as well as the affected area around the cyclone (marked as the 34-kt isotach) with shading according to the number of pixels overlapping. Inside, there is an inset with the full track and the region of study marked with a red box. Ophelia track is divided in three phases: Genesis (triangles), maturing (squares) and mature (stars). Histograms show induced chl-a (b) and SST anomalies (c), by phase of the storm (colours) and general (grey).

For the case study of Hurricane Ophelia (2017), three different phases of the storm were studied, corresponding approximately to: cyclogenesis (Fig. 6a, triangles), maturing (Fig. 6a, squares), mature hurricane (Fig. 6a, stars). There are 23 total observations; the first two phases encompass 8 observations and the last 7. Each of these phases has its own histogram in Figs. 6b and 6c (shown in colours), for the induced chl-a and SST anomalies, respectively. The histograms are inserted in a larger one (in grey), representing the total induced anomalies caused by Ophelia and therefore, the sum of all three will result in the bigger one. Regarding the chl-a induced anomalies (Fig. 6b), Ophelia seemed to have a higher impact towards the end of its track in the region of study, when the storm had the highest intensity and the mean values of the induced anomalies increased along the track. Even at the storm's genesis, the induced anomalies were mostly positive with a mean value of +0.016 mg/m^3 reaching +0.030 mg/m^3 in the most intense phase. In contrast, the SST induced anomalies (Fig. 6c) present the highest mean response (-1.972 K) at the initial phase. The SST induced anomaly is then seen decreasing as the storm goes on, with the last phase weighing the most in the general distribution (as was seen for the chl-a). The highest impact of the storm during the initial phases may reflect that this is the phase of the storm with highest interaction with the ocean, regarding thermodynamic exchanges (Emanuel, 2003).

https://doi.org/10.5194/egusphere-2022-31
Preprint. Discussion started: 10 March 2022

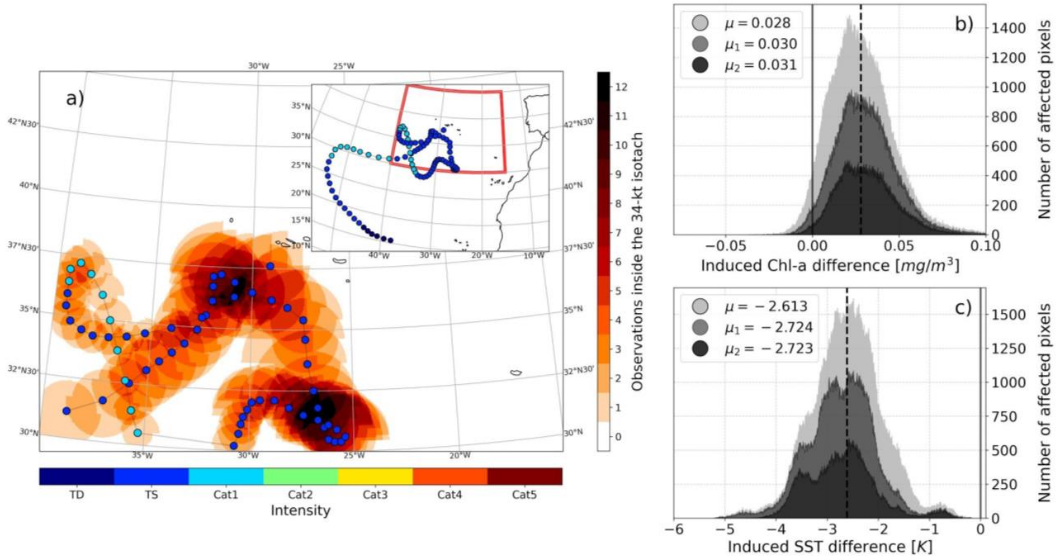

Figure 7 - Case study for Hurricane Nadine, in 2012, with the right panel the same as in Fig. 6. For Nadine, histograms b) and c) pertain to the induced chl-a and SST anomalies, respectively, based on the amount of overlap verified in each pixel: soft grey – No overlap; Dark grey – 3-pixel overlap; Black – 5-pixel overlap.

Hurricane Nadine's (2012) case study shows very different behaviour and impact during its lifetime to that of Hurricane Ophelia. In this case, histograms represent differently impacted areas, with the darker histograms (Figs. 7b and 7c) corresponding to the areas with more overlaid observations (as seen in Fig. 7a). The threshold chosen for analysis were 3 overlaid observations for the middle shade and 5 for the darkest one, with the biggest histogram showing the general induced anomalies for Hurricane Nadine. The conclusions drawn regarding the chl-a and SST induced anomalies are similar in this case study: The more time the TC spent over a certain area the more this area became affected by its passage, with large anomalies registered in both variables (over 0.031 mg/m^3 and -2.723 K for chl-a and SST, respectively). This shows that the TC intensity is somewhat irrelevant given that the geometry of its track is ideal to stay longer over a region. With this in mind, it is possible to hypothesise that the translation speed also had a relevant role in these results, with a slower TC (Nadine was one of the slowest TCs in this study, as seen by the closer observations in Fig. 7a and by Figs. 5c and 5f) spending more time over a region and therefore producing larger anomalies.

Final remarks

The current study provides the first general assessment of the bio-physical oceanic response to the passage of TCs in a relatively low cyclonic activity area such as the region near the Azores archipelago. It is important to stress the efficiency of identifying the precise timing and associated spatial impacts of all TCs using remotely sensed products that rely on interpolated areas to fill existing gaps due to cloud coverage or lack of satellite imagery.

https://doi.org/10.5194/egusphere-2022-31
Preprint. Discussion started: 10 March 2022

Over the Azores region, it was generally identified the existence of a bio-physical response after the passage of a TC from the analysis of chl-a and SST datasets, which produced signatures of positive (chl-a) and negative (SST) anomalies, for a period of about two weeks after the passage of a TC. This signature is considerably more intense for the SST analysis, in which the passage of a TC results in nearly all observed pixels to have a negative (i.e., cooling) induced anomaly. On average, TCs produced positive anomalies in the order of 0.026 mg/m^3 regarding chl-a and a cooling of 1.554 K.

The more powerful TCs tend to produce more intense bio-physical oceanic responses which agree with previous literature on the topic (Chacko, 2019; Price, 1981; Price et al., 1994). The TCs translation speed was also confirmed to be relevant in inducing anomalies in both variables, although in this instance the direct relation was not confirmed since results were not significant at the 95 % statistical confidence level. The impacted area was also found to be significantly linked to the oceanic response. However, the sensitivity to the impacted area can rise due to several other factors: slower TCs impact larger areas (due to track geometry); more intense TCs impact larger areas (Knaff et al., 2014); and TCs nearing post-tropical transition are generally larger (Knaff et al., 2014). These effects, either individually or combined, can affect the induced anomalies at different levels.

Two particular case studies were evaluated in further detail concerning hurricanes Ophelia (2017) and Nadine (2012). Hurricane Ophelia was a particular case as it corresponds to the only major hurricane in this study region and had almost its entire track inside this area. Ophelia showed strong induced anomalies for both chl-a and SST variables. Regarding chl-a, Ophelia had a stronger impact towards the end of its track within the region, revealing that its intensity played a key role in inducing chl-a anomalies. On the other hand, Ophelia had a stronger impact on the SST in its cyclogenesis, probably related to ocean-atmosphere thermodynamic exchanges during its maturing. Hurricane Nadine, one of the slowest TCs in this study, showed more prominent anomalies, especially regarding SST. In this case, considering the low translational speed of Nadine, the objective was to study the impact that consecutive overlaid observations had on the induced anomalies. It is evident through this analysis that the impact increases with the number of overlaid observations, implying that Nadine’s slow translation speed and particular track geometry played a key role in creating such anomalies.

This study allowed for both the quality control of the remotely sensed “cloud-free” chl-a and SST multi-sensor products, in the sense that it identified expected changes in the variables in areas covered by TC clouds and established crucial relations with some principal TC aspects. Future studies should aim to understand the inherent physical mechanisms that affect the ocean during and after the passage of a TC to better comprehend the associated induced anomalies.

Code and Data availability

All code and raw data used to support the conclusion of this article will be made available by the authors, without undue reservation.

https://doi.org/10.5194/egusphere-2022-31
Preprint. Discussion started: 10 March 2022

Acknowledgements

Research by Miguel M. Lima was supported by the Portuguese Science Foundation (FCT) through the project "DiscoverAZORES", PTDC/CTA-AMB/28511/2017.

Author Contribution

Miguel M. Lima: Conceptualization, methodology, software, validation, formal analysis, investigation, writing – original draft, review & editing. Célia M. Gouveia: Validation, supervision, writing – review & editing. Ricardo M. Trigo: Validation, supervision, writing – review & editing, funding acquisition.

Declaration of Interests

The authors declare that they have no known competing financial interests or personal relationships that could have appeared to influence the work reported in this paper.

References

Amorim, P., Perán, A. D., Pham, C. K., Juliano, M., Cardigos, F., Tempera, F., & Morato, T. (2017). Overview of the ocean climatology and its variability in the Azores region of the North Atlantic including environmental characteristics at the seabed. *Frontiers in Marine Science*, *4*, 56. doi:10.3389/fmars.2017.00056

Baatsen, M., Haarsma, R. J., Van Delden, A. J., and de Vries, H. (2015). Severe Autumn Storms in Future Western Europe with a Warmer Atlantic Ocean. Clim. Dyn. 45 (3-4), 949–964. doi:10.1007/s00382-014-2329-8

Celisse, A., Marot, G., Pierre-Jean, M., & Rigaill, G. J. (2018). New efficient algorithms for multiple change-point detection with reproducing kernels. Computational Statistics & Data Analysis, 128, 200-220. doi:10.1016/j.csda.2018.07.002

Chen, S., Elsberry, R. L., & Harr, P. A. (2017). Modeling interaction of a tropical cyclone with its cold wake. *Journal of the Atmospheric Sciences*, *74*(12), 3981-4001. doi:10.1175/JAS-D-16-0246.1

Chacko, N. (2019). Differential chlorophyll blooms induced by tropical cyclones and their relation to cyclone characteristics and ocean pre-conditions in the Indian Ocean. *Journal of Earth System Science*, *128*(7), 1-11. doi:10.1007/s12040-019-1207-5

CMEMS. (2021a). ESA SST CCI and C3S reprocessed sea surface temperature analyses. Retrieved from https://resources.marine.copernicus.eu/?option=com_csw&view=details&product_id=SST_GLO_SST_L4_REP_OBSERVATIONS_010_024

CMEMS. (2021b). Global ocean chlorophyll, PP and PFT (copernicus-globcolour) from satellite observations: Monthly and daily interpolated (reprocessed from 1997). Retrieved from

https://doi.org/10.5194/egusphere-2022-31
Preprint. Discussion started: 10 March 2022

https://resources.marine.copernicus.eu/?option=com_csw&view=details&product_id=OCEANCOLOUR_GLO_CHL_L4_REP_OBSERVATIONS_009_082

Dickey, T., Frye, D., McNeil, J., Manov, D., Nelson, N., Sigurdson, D., ... & Johnson, R. (1998). Upper-ocean temperature response to Hurricane Felix as measured by the Bermuda Testbed Mooring. *Monthly Weather Review*, *126*(5), 1195-1201. doi:10.1175/1520-0493(1998)126<1195:UOTRTH>2.0.CO;2

Donlon, C. J., Martin, M., Stark, J., Roberts-Jones, J., Fiedler, E., & Wimmer, W. (2012). The operational sea surface temperature and sea ice analysis (OSTIA) system. Remote Sensing of Environment, 116, 140-158. doi:10.1016/j.rse.2010.10.017

Emanuel, K. (2003). Tropical Cyclones. Annu. Rev. Earth Planet. Sci. 31 (1), 75–104. doi:10.1146/annurev.earth.31.100901.141259

Garnesson, P., Mangin, A., Fanton d'Andon, O., Demaria, J., & Bretagnon, M. (2019). The CMEMS GlobColour chlorophyll a product based on satellite observation: multi-sensor merging and flagging strategies. Ocean Science, 15(3), 819-830. doi:10.5194/os-15-819-2019

Good, S., Fiedler, E., Mao, C., Martin, M. J., Maycock, A., Reid, R., ... & Worsfold, M. (2020). The current configuration of the OSTIA system for operational production of foundation sea surface temperature and ice concentration analyses. *Remote Sensing*, *12*(4), 720. doi:10.3390/rs12040720

Haarsma, R. J., Hazeleger, W., Severijns, C., de Vries, H., Sterl, A., Bintanja, R., et al. (2013). More Hurricanes to Hit Western Europe Due to Global Warming. Geophys. Res. Lett. 40, 1783–1788. doi:10.1002/grl.50360

Hart, R. E., & Evans, J. L. (2001). A climatology of the extratropical transition of Atlantic tropical cyclones. Journal of Climate, 14(4), 546-564. doi:10.1175/1520-0442(2001)014<0546:ACOTET>2.0.CO;2

Holton, J. R., and Hakim, G. J. (2012). An Introduction to Dynamic Meteorology. 5th ed., Vol. 88. San Diego, CA: Academic Press, Elsevier. doi:10.1119/1.1987371

Kawai, Y., & Wada, A. (2011). Detection of cyclone-induced rapid increases in chlorophyll-a with sea surface cooling in the northwestern Pacific Ocean from a MODIS/SeaWiFS merged satellite chlorophyll product. *International journal of remote sensing*, *32*(24), 9455-9471. doi:10.1080/01431161.2011.562252

Knaff, J. A., Longmore, S. P., & Molenar, D. A. (2014). An objective satellite-based tropical cyclone size climatology. *Journal of Climate*, *27*(1), 455-476. doi:10.1175/JCLI-D-13-00096.1

Knapp, K. R., Kruk, M. C., Levinson, D. H., Diamond, H. J., and Neumann, C. J. (2010). The International Best Track Archive for Climate Stewardship (IBTrACS). Bull. Amer. Meteorol. Soc. 91 (3), 363–376. doi:10.1175/2009BAMS2755.1

https://doi.org/10.5194/egusphere-2022-31
Preprint. Discussion started: 10 March 2022

Kossin, J. P., Knapp, K. R., Olander, T. L., and Velden, C. S. (2020). Global Increase in Major Tropical Cyclone Exceedance Probability over the Past Four Decades. Proc. Natl. Acad. Sci. USA 117 (22), 11975–11980. doi:10.1073/pnas.1920849117

Krasnopolsky, V., Nadiga, S., Mehra, A., Bayler, E., & Behringer, D. (2016). Neural networks technique for filling gaps in satellite measurements: Application to ocean color observations. Computational intelligence and neuroscience, 2016. doi:10.1155/2016/6156513

Lavergne, T., Sørensen, A. M., Kern, S., Tonboe, R., Notz, D., Aaboe, S., ... & Pedersen, L. T. (2019). Version 2 of the EUMETSAT OSI SAF and ESA CCI sea-ice concentration climate data records. *The Cryosphere*, *13*(1), 49-78. doi:10.5194/tc-13-49-2019

Lima, M. M. , Hurduc, A., Ramos, A. M. and Trigo, R. M. (2021). The Increasing Frequency of Tropical Cyclones in the Northeastern Atlantic Sector. Front. Earth Sci. 9:745115. doi: 10.3389/feart.2021.745115

Liu, X., Wang, M., & Shi, W. (2009). A study of a Hurricane Katrina–induced phytoplankton bloom using satellite observations and model simulations. *Journal of Geophysical Research: Oceans*, *114*(C3). doi:10.1029/2008JC004934

Maneesha, K., Murty, V. S. N., Ravichandran, M., Lee, T., Yu, W., & McPhaden, M. J. (2012). Upper ocean variability in the Bay of Bengal during the tropical cyclones Nargis and Laila. *Progress in Oceanography*, *106*, 49-61. doi:10.1016/j.pocean.2012.06.006

Merchant, C. J., Le Borgne, P., Roquet, H., & Legendre, G. (2013). Extended optimal estimation techniques for sea surface temperature from the Spinning Enhanced Visible and Infra-Red Imager (SEVIRI). *Remote Sensing of Environment*, *131*, 287-297. doi:10.1016/j.rse.2012.12.019

Pan, J., Huang, L., Devlin, A. T., & Lin, H. (2018). Quantification of typhoon-induced phytoplankton blooms using satellite multi-sensor data. *Remote Sensing*, *10*(2), 318. doi:10.3390/rs10020318

Pearce, R. P. (1987). The physics of hurricanes. Physics in Technology, 18(5), 215.

Price, J. F. (1981). Upper ocean response to a hurricane. *Journal of Physical Oceanography*, *11*(2), 153-175. doi:10.1175/1520-0485(1981)011<0153:UORTAH>2.0.CO;2

Price, J. F., Sanford, T. B., & Forristall, G. Z. (1994). Forced stage response to a moving hurricane. *Journal of Physical Oceanography*, *24*(2), 233-260. doi:10.1175/1520-0485(1994)024<0233:FSRTAM>2.0.CO;2

Ramsay, H. (2017). The Global Climatology of Tropical Cyclones. Oxford Research Encyclopedia of Natural Hazard Science. Victoria, Austrália: Oxford University Press. doi:10.1093/acrefore/9780199389407.013.79

Saulquin, B., Gohin, F., & Fanton d'Andon, O. (2019). Interpolated fields of satellite-derived multi-algorithm chlorophyll-a estimates at global and European scales in the frame of the European Copernicus-Marine Environment Monitoring Service. Journal of Operational Oceanography, 12(1), 47-57. doi:10.1080/1755876X.2018.1552358

Shropshire, T., Li, Y., & He, R. (2016). Storm impact on sea surface temperature and chlorophyll a in the Gulf of Mexico and Sargasso Sea based on daily cloud-free satellite data reconstructions. *Geophysical Research Letters*, *43*(23), 12-199. doi:10.1002/2016GL071178

Subrahmanyam, B., Rao, K. H., Srinivasa Rao, N., Murty, V. S. N., & Sharp, R. J. (2002). Influence of a tropical cyclone on chlorophyll-a concentration in the Arabian Sea. *Geophysical Research Letters*, *29*(22), 22-1. doi:10.1029/2002GL015892

Taylor, H. T., Ward, B., Willis, M., & Zaleski, W. (2010). The saffir-simpson hurricane wind scale. Atmospheric Administration: Washington, DC, USA.

Truong, C., Oudre, L., & Vayatis, N. (2020). Selective review of offline change point detection methods. Signal Processing, 167, 107299. doi:10.1016/j.sigpro.2019.107299

Walker, N. D., Leben, R. R., & Balasubramanian, S. (2005). Hurricane-forced upwelling and chlorophyll-a enhancement within cold-core cyclones in the Gulf of Mexico. *Geophysical Research Letters*, *32*(18). doi:10.1029/2005GL023716

Zhang, J., Lin, Y., Chavas, D. R., & Mei, W. (2019). Tropical cyclone cold wake size and its applications to power dissipation and ocean heat uptake estimates. *Geophysical Research Letters*, *46*(16), 10177-10185. doi:10.1029/2019GL083783

Zheng, Z. W., Ho, C. R., & Kuo, N. J. (2008). Importance of pre-existing oceanic conditions to upper ocean response induced by Super Typhoon Hai-Tang. *Geophysical Research Letters*, *35*(20). doi:10.1029/2008GL035524